Phosphorylation of Serine 392 Stabilizes the Tetramer Formation of Tumor Suppressor Protein p53

Kazuyasu Sakaguchi,*,‡ Hiroshi Sakamoto,‡ Marc S. Lewis,§ Carl W. Anderson,|| John W. Erickson,⊥ Ettore Appella,‡ and Dong Xie⊥

Laboratory of Cell Biology, National Cancer Institute, and Biomedical Engineering and Instrumentation Program, National Center for Research Resources, National Institutes of Health, Bethesda, Maryland 20892, Brookhaven National Laboratory, Upton, New York 11973, and Structural Biochemistry Program, National Cancer Institute−Frederick Cancer Research and Development Center, Frederick, Maryland 21702

Received April 1, 1997; Revised Manuscript Received June 6, 1997⊗

ABSTRACT: Tumor suppressor protein p53 is a tetrameric phosphoprotein that activates transcription from several cell cycle regulating genes in response to DNA damage. Tetramer formation is critical to p53's ability to activate transcription; however, posttranslational modifications and protein stabilization also contribute to p53's ability to activate transcription. To determine if phosphorylation affects tetramer formation, we synthesized phosphopeptides corresponding to residues 303−393 of human p53, which includes the domain responsible for tetramer formation. Phosphate was chemically incorporated at Ser315, Ser378, or Ser392 and also at both Ser315 and Ser392. Equilibrium ultracentrifugal analyses showed that phosphorylation at Ser392 increased the association constant for reversible tetramer formation nearly 10-fold. Phosphorylation of either Ser315 or Ser378 had little effect on tetramer formation, but phosphorylation of Ser315 largely reversed the effect of phosphorylation at Ser392. Analyses by calorimetry demonstrated that phosphorylation may influence subunit affinity (and, in turn, DNA binding) by an enthalpy-driven process, possibly between the C-terminal residues and the region immediately adjacent to Ser315. The K_d for the tetramer−monomer transition of the unphosphorylated p53 C-terminal domain was determined to be ∼1−10 μM. Thus, in normal, undamaged cells p53 may be largely monomeric. Enhancement of tetramer formation through phosphorylation of Ser392, coupled with a DNA-damage-induced increase in its nuclear concentration, could provide a switch that activates p53 as a transcription factor in response to DNA damage.

The tumor suppressor protein p53 is a 393 amino acid transcriptional enhancer phosphoprotein that reversibly associates to form tetramers. Functional inactivation of the protein either by association with viral products or by mutations in the p53 gene leads to cellular transformation (*1*). In response to damaged DNA, mammalian cell growth is arrested at cell cycle checkpoints (*2*−*4*), and under some circumstances, DNA damage initiates apoptosis (*5, 6*). Recent studies have shown that the p53 tumor suppressor protein is an essential component of the G1 checkpoint pathway (*7*); however, it also modulates the initiation of apoptosis (*8*). These functions account, at least in part, for the importance of p53 in suppressing or eliminating preneoplastic or neoplastic cells. In turn, p53 function is mediated through its physical characteristics, and these may be modulated by posttranslational mechanisms (*9, 10*). Thus, biophysical studies of p53 and its functional domains are fundamental to an understanding of those properties that are important for normal p53 function.

Wild-type p53 protein forms tetramers and higher order oligomeric structures in solution (*11*), and the domain responsible for oligomerization was localized to the carboxyl terminus (*12*). Subsequent studies showed that amino acids 319−360 were sufficient for the formation of recombinant protein tetramers (*13*−*15*). Recently, the three-dimensional structure of the core tetramerization domain was determined by using multidimensional NMR spectroscopy and X-ray crystallography (*16*−*19*). Each monomer is composed of a turn (Asp324−Gly325), a β-strand (Glu326−Arg333), another turn (Gly334), and an α-helix (Arg335−Gly356). Two monomer peptides form a dimer in which the α-helices and β-strands are antiparallel. Two dimers interact to form a tetramer through their α-helices. The β-strands lie on the outside of the tetramer on opposite faces. Thus, the tetramer is best described as a dimer of dimers, with the two dimers interacting through their α-helices to form a four-helix bundle. Although the role of tetramerization in p53 function is not completely understood, it is required for efficient site-specific DNA binding and contributes to p53's ability to activate transcription from natural promoters (*20, 21*).

Carboxy-terminal p53 sequences appear to have an inhibitory effect on site-specific DNA binding (*22*). Wild-type p53 made in *Escherichia coli* binds relatively poorly to the p53 consensus recognition sequence, but its binding is enhanced by several treatments that affect the carboxyl terminus. These include deletion of 30 carboxy-terminal residues (*22*), complex formation with antibodies or other

* To whom correspondence should be addressed: Laboratory of Cell Biology, National Cancer Institute, Bldg. 37, Rm. 1B10, 37 Convent Dr., MSC 4255, Bethesda, MD 20892. Tel (301) 496-4549; Fax (301) 496-7220; e-mail: kazuyasu@helix.nih.gov.

‡ National Cancer Institute, NIH.

§ National Center for Research Resources, NIH.

|| Brookhaven National Laboratory.

⊥ NCI-FCRDC.

⊗ Abstract published in *Advance ACS Abstracts,* August 1, 1997.

S0006-2960(97)00759-9 CCC: $14.00

proteins that recognize carboxy-terminal sequences (*22*, *23*), and phosphorylation by casein kinase II (CKII)[1] and protein kinase C (PKC) (*22*, *24*, *25*). CKII phosphorylates the penultimate residues of mouse and human p53, Ser389 and Ser392, respectively (*10*, *26*). Serine 312 (murine) and serine 315 (human) also are phosphorylated *in vivo*, and these residues can be phosphorylated *in vitro* by the $p34^{cdc2}$ cyclin-dependent kinase (*27*−*29*). Serine 378 is phosphorylated *in vitro* by PKC (*25*). The last 27 residues of human p53 are encoded by a separate exon, suggesting that this segment may comprise a distinct functional domain (*30*). Enhancement of DNA binding by modification of this C-terminal negative regulatory domain is an important step in the activation of p53 protein. The carboxy terminus is high in basic residues and provides non-sequence-specific DNA binding and strand annealing activities that are independent of the sequence-specific DNA binding central domain (*12*, *15*, *31*, *32*).

Because wild-type p53 normally is phosphorylated, it is important to determine how phosphorylation affects the thermodynamic aspects of tetramer formation. Accordingly, using a fragment condensation method, we synthesized the unphosphorylated p53 peptide encompassing Ser303−Asp393 as well as phosphopeptides with phosphate incorporated at Ser315, at Ser378, or at Ser392, and we investigated the thermodynamics of reversible tetramer formation by these peptides using equilibrium analytical ultracentrifugation and microcalorimetry.

EXPERIMENTAL PROCEDURES

Peptide Synthesis. The p53 peptides were synthesized by a segment condensation method using appropriate peptide thioesters (*33*). Peptide thioesters, corresponding to residues 303−334, [$Ser(PO_2H)^{315}$]303−334, and 335−360, were synthesized with *t*-Boc chemistry using *t*-Boc-Gly-SCH_2CH_2-CO-Ala-MBHA (4-methyl benzhydrylamine) resin and cleaved by HF−*p*-cresol. After all of the lysine side chains of the peptides were protected by *t*-Boc groups, the peptide thioesters were successively condensed with the C-terminal portion (sequences 361−393 with phosphoserine at 378 or 392) in dimethyl sulfoxide (DMSO) in the presence of $AgNO_3$ and *N*-hydroxysuccinimide. Deprotection of the final peptides was accomplished using trifluoroacetic acid−ethanedithiol.

All the synthetic peptides were purified by HPLC on a Vydac C-4 column with 0.05% trifluoroacetic acid/water−acetonitrile and their composition and mass were confirmed by amino acid analysis and mass spectroscopy. The extinction coefficients were determined by quantitative amino acid analysis.

Analytical Ultracentrifugation. Analytical ultracentrifugation was carried out using a Beckman XL-A analytical ultracentrifuge with a four-place titanium rotor and carbon-filled epoxy double-sector centerpieces in the cells. Tris·HCl, pH 7.5 (50 mM), with 100 mM NaCl was used as a buffer. Rotor speeds were in the range of 25 000 rpm. With column lengths of approximately 5 mm, time-invariant scans were obtained by 72 h. All scans were performed at 230 nm. The data were edited using the XL-A software and analyzed by mathematical modeling using MLAB (Civilized Software, Bethesda, MD) to perform nonlinear least-squares curve-fitting of the data with appropriate mathematical models.

The mathematical model for fitting the data has the form

$$A_r = A_{b,1}\exp[AM_1(r^2 - r_b^2)] + A_{b,1}^4\exp[\ln k_{14} + 4AM_1(r^2 - r_b^2)] + \epsilon$$

A_r refers to the total absorbance as a function of radial position. $A_{b,1}$ is the absorbance of monomer at r_b, the radial position from the cell bottom. $A = (1 - \phi^*\rho)\omega^2/2RT$, where ϕ^* is the compositional partial specific volume of the peptide, ρ is the solvent density, ω is the angular velocity of the rotor, R is the gas constant, and T is the absolute temperature. M_1 is the molecular mass of the monomer, and ϵ is a small baseline error correction term.

This model is written in terms of an equilibrium constant on an absorbance concentration scale, where $k_{14} = A_4/A_1^4$; for thermodynamic calculations this equilibrium constant must be converted to a molar scale by using $\ln K_{14} = \ln k_{14} + \ln (E_1^3/4)$, where E_1 is the molar extinction coefficient of the peptide monomer at 230 nm. This relationship assumes that $E_4 = 4E_1$. The change of standard free energy of the association is then given by $\Delta G^\circ = -RT \ln K_{14}$. This model also assumes that the apparent partial specific volumes of the monomer and the tetramer are identical. The values of M_1 and ϕ^* were calculated from the amino acid sequence of the peptides for a temperature of 25 °C, using the values of Perkins (*34*). The values of ϕ^* at 30 °C were calculated by using a value of 0.000345 $cm^3 \cdot g^{-1} \cdot deg^{-1}$ for $\Delta\phi^*/\Delta T$. The values of the density of the buffer were calculated from standard density tables.

Isothermal Titration Calorimetry. The heats of tetramer dissociation were measured with a Omega titration microcalorimeter (Microcal, Northampton, MA). The design and operation of this instrument have been previously described (*35*). Peptide solutions were prepared by overnight dialysis at 4 °C against 50 mM sodium phosphate buffer at pH 7.5 with 0.1 M NaCl. Concentrations were determined by measuring absorbance at 280 nm using an extinction coefficient of 1100 M^{-1}. All samples were degassed for 20 min prior to titration. The peptide concentrations were approximately 250 μM for both the SS and SP peptides; the predominant oligomeric state is tetramer at this concentration. At each of the different temperatures, aliquots of 5−10 μL of concentrated protein solution were injected into the buffer-containing calorimeter cell and the heat changes were recorded. For the statistical thermodynamic analysis of the ITC data, we developed a nonlinear least-squares fitting program, which was incorporated into the Igor software package (WaveMetrics, Inc., Lake Oswego, OR).

Differential Scanning Calorimetry. The DSC experiments were performed using a Nano-DSC (Calorimetry Sciences Corp., Provo, UT) (*36*). The peptide samples were prepared as for the ITC experiment. Both peptide concentrations were 100 μM. A typical DSC experiment includes three scans: a scan of buffer, which is used as baseline, a scan of the peptide sample, and a rescan of the peptide sample after the sample was rapidly cooled from the first scan. The reproducibility of the baseline was checked by running multiple scans of the buffer. In all cases the reproducibility was better than 15 μcal/°C. The reversibility of the temperature-induced denaturation of p53 peptides was verified

[1] Abbreviations: CKII, casein kinase II; PKC, protein kinase C; ITC, isothermal titration calorimetry; DSC, differential scanning calorimetry.

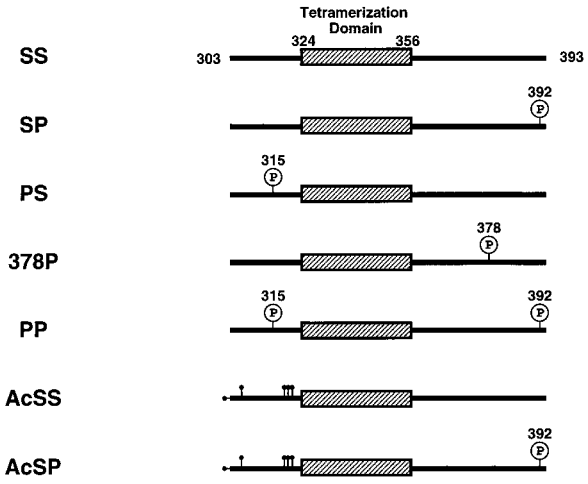

FIGURE 1: Diagram of the synthetic peptides showing the location of the tetramerization domain and the locations of the phosphorylated serines and the acetylated groups. Dot (●) and P in circle represent the acetyl and phosphate groups, respectively.

Table 1: Standard Free Energy and Dissociation Constant for Tetramer Formation of p53(303−393) Peptides at 30 °C by Ultracentrifugal Analysis

peptide	$\Delta G°^a$ (kcal/mol)	$K_d{}^b$ (μM)	RA^c
SS	-22.9 ± 0.1	3.84	1.00
SP	-26.7 ± 0.2	0.487	7.89
PS	-23.3 ± 0.2	3.25	1.18
378P	-23.1 ± 0.1	3.60	1.07
PP	-23.7 ± 0.3	2.49	1.54
AcSS	-22.6 ± 0.1	4.54	0.85
AcSP	-22.5 ± 0.1	4.85	0.79

[a] The standard errors of $\Delta G°$ have been calculated from the standard errors of ln K_{14} obtained by fitting the data. [b] The dissociation constant is calculated by $K_d = (K_{14}/2)^{-1/3}$. [c] Relative affinity with SS = 1.

by comparing the transition enthalpy of the first scan and the rescan. Both the SS and SP peptides exhibited 95−100% reversibility. In order to ascertain that the observed transition is an equilibrium process, we also carried out experiments at different scan rates (1 and 2 °C/min). All thermodynamic parameters associated with the transitions were scan-rate-independent. This validates the thermodynamic analysis of the experimental data. The data analysis consisted of two steps: subtraction of the buffer baseline and normalization to the tetramer molar concentration. The analysis was performed using the program C_p calc (Calorimetry Sciences Corp.).

RESULTS

To determine whether or not phosphorylation affects tetrameric formation, we synthesized chemically two unphosphorylated and five phosphorylated peptides, comprising human p53 Ser303−Asp393 by a fragment condensation method (*33*). Phosphate was incorporated at Ser315, Ser378, or Ser392 and at both Ser315 and Ser392 (Figure 1).

Analytical Ultracentrifugation. The reversible tetramer formation of p53 C-terminal peptides (residues 303−393) was analyzed by equilibrium analytical ultracentrifugation. Table 1 shows the free energy for tetramer formation of the peptides in Tris buffer, pH 7.5, at centrifugal equilibrium at 28 000 rpm at 30 °C. Table 1 also presents the corresponding values of K_d and the relative affinities of tetramerization with respect to the unphosphorylated peptide (peptide SS). All of the peptides with either one or two phosphoserines (peptides SP, PS, 378P, and PP) exhibited the same type of monomer-tetramer equilibrium as the unphosphorylated peptide. No formation of either higher oligomers or dimers with any peptides was detected by mathematical modeling of the data. Our analyses showed that phosphorylation of Ser392 (peptide SP) enhanced formation of the p53(303−393) tetramer with an increase in the magnitude of $\Delta G°$ of almost 4 kcal/mol at 30 °C. This increase in the magnitude of the free energy attributable to phosphorylation corresponds to a nearly 10-fold decrease of the dissociation constant of tetramer formation (Table 1). On the other hand, phosphorylation of Ser315 (peptide PS) or Ser 378 (peptide 378P) had no significant effect on tetramer formation. Phosphorylation of both Ser315 and Ser392 (peptide PP) resulted in essentially the same association constant as that obtained for the unphosphorylated peptide. The value of $\Delta G°$ of PP at 30 °C is 3 kcal/mol more positive than that of the SP peptide. This result suggests that the phosphoserine at residue 392 could be interacting with the residue(s) in the vicinity of Ser315 and that phosphorylation at Ser315 interferes with this interaction. Because the p53 peptide tetramer is a dimer of dimers with an antiparallel orientation, the *N*-terminal flanking region can be very close to the C-terminal phosphorylated site.

In order to determine the effect of the amino groups located in the *N*-terminal region of the p53 peptide on the interaction of peptide with phosphorylated Ser392, these amino groups were blocked by acetylation. The α-amino group and four lysine side-chain groups at positions 305, 319, 320, and 321 were acetylated in the peptides AcSS and AcSP. AcSS was unphosphorylated and AcSP had Ser392 phosphorylated. Table 1 also presents the result demonstrating the effect of the blocking of the amino groups with and without Ser392 phosphorylation. Acetylation of the amino groups in the *N*-terminal region completely eliminated the enhancement of tetramerization by phosphorylation of Ser392, while acetylation itself had a minimal effect on the formation of tetramers by the unphosphorylated peptide. The value of $\Delta G°$ at 30 °C of AcSP was 4.2 kcal/mol more positive than that of the SP peptide, while the value of $\Delta G°$ at 30 °C of AcSS was almost the same as that of SS. These results do suggest that the phosphoserine at position 392 might interact with other residues in the vicinity of Ser315.

Isothermal Titration Calorimetry and Statistical Thermodynamic Analysis. Figure 2 shows a typical calorimetric titration curve in which aliquots of 7 μL of 258 μM p53 SS peptide were injected into buffer at 60 °C with a time interval of 8 min between the injections. In order to obtain the thermodynamic parameters characterizing the dissociation of the p53 peptides, we used a model that describes the reversible equilibrium between tetramer and monomer:

$$P_4 \leftrightarrow 4P_1 \quad (1)$$

The equilibrium constant for dissociation is defined in the standard way as

$$K = C_1{}^4/C_4 = \exp(-\Delta G°/RT) \quad (2)$$

where C_1 and C_4 are the molar concentrations of monomer and tetramer, respectively. $\Delta G°$ is the change of the standard free energy of dissociation, defined as

Table 2: Thermodynamic Parameters of p53 Tetramer Dissociation as a Function of Temperature[a] by Isothermal Titration Calorimetry

	temp (°C)	ΔH^b (kcal/mol)	ΔS^c [cal/(mol·K)]	$\Delta C_p{}^d$ [kcal/(mol·K)][d]	ΔG^b (kcal/mol)	K_d (μM)
SS	65.0	34.6 ± 0.6	36.7		22.2 ± 0.4	20.8
	59.8	28.4 ± 0.9	15.3		23.3 ± 0.2	10.0
	45.1	3.4 ± 0.2	−67.2		24.8 ± 0.2	2.6
	37.0	−9.3	−111.4		25.3	1.5
	30.0	−20.3	−150.0	1.6 ± 0.2	25.2	1.2
SP	67.4	59.4 ± 2.4	103.5		24.1 ± 0.1	8.6
	65.1	55.9 ± 1.2	93.8		24.2 ± 0.2	7.8
	60.0	44.8 ± 6.0	57.5		25.6 ± 0.1	3.1
	55.0	33.6 ± 2.1	24.6		25.5 ± 0.2	2.7
	37.0	−3.5	−98.8		27.2	0.5
	30.0	−18.8	−151.4	2.1 ± 0.2	27.1	0.4

[a] The values at 37 and 30 °C were calculated using eq 7 and the experimental data at higher temperatures. The buffer was 50 mM sodium phosphate, pH 7.5, with 0.1 M NaCl. [b] The errors of ΔH and ΔG were calculated from nonlinear least-squares fitting. [c] The ΔS values were calculated by using the formula $\Delta S = (\Delta H - \Delta G)/T$. [d] The values of ΔC_p were determined by the temperature dependence of ΔH as shown in Figure 3.

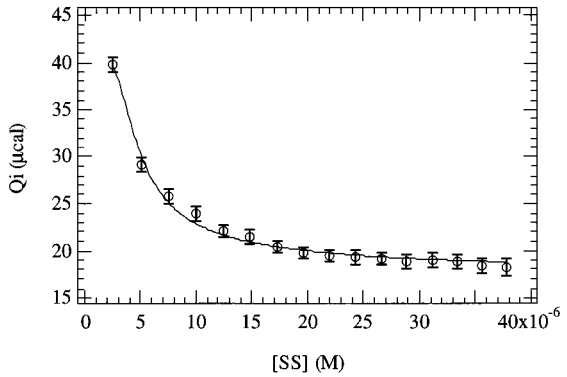

FIGURE 2: Heat of injection of p53 SS peptide into buffer at 60 °C. The *x*-axis corresponds to the concentration of SS peptide in the calorimeter cell. Each point corresponds to the injection heat of 7 μL of 258 μM SS peptide at 8-min time intervals. The last few points correspond to the heat of dilution since no further tetramer dissociation occurs at those concentrations. The solid line represents the best-fitting curve using a tetramer to monomer dissociation model as discussed in the text. The binding is characterized by an enthalpy of 28.4 kcal/mol and a dissociation constant of 10.0 μM.

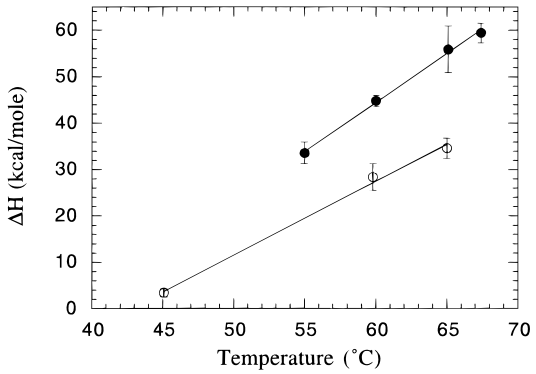

FIGURE 3: Temperature dependence of the tetramer dissociation enthalpy of p53 SS and SP peptides. The filled circles represent the data for the SP peptide; the open circles are for the SS peptide. The values of ΔC_p determined from this figure, according to eq 7a, were 2.1 kcal/(mol·K) for the SP peptide and 1.6 kcal/(mol·K) for the SS peptide, respectively.

$$\Delta G^\circ = \Delta H^\circ - T\Delta S^\circ \tag{3}$$

where ΔH° and ΔS° are the standard molar enthalpy and entropy changes of dissociation. The total protein concentration, C_T, can be expressed as

$$C_T = 4C_4 + C_1 \tag{4}$$

Rearranging eqs 2 and 4 gives

$$4C_1{}^4 + KC_1 - KC_T = 0 \tag{5}$$

The numerical solution of this equation gives the value of C_1 as a function of the equilibrium constant and the total protein concentration.

The reaction heat of the *i*th injection, Q_i, is represented as

$$Q_i = \Delta H[V_c(C_i - C_{i-1}) - V'C']/4 + \Delta H_d \tag{6}$$

where ΔH is the change of tetramer dissociation enthalpy, V_c is the calorimeter cell volume, C_i and C_{i-1} are monomer concentration in the calorimeter cell after the *i*th and $(i-1)$th injection, respectively, V' and C' are the injection volume and the monomer concentration of the sample in the injection syringe, and ΔH_d is the mixing heat of the p53 molecule, representing the baseline heat of injection. Similar analyses of tetramer folding/unfolding equilibria and dimer−monomer equilibria have been described (*37*, *38*).

In this work, all ITC experimental data can be accurately described by the monomer−tetramer model. One example of the data fitting is shown in Figure 2. The good agreement between this model and the experimental data also suggests that it is quite improbable that there is a significant dimer concentration. We have also tested the possibility of a dimer to monomer dissociation model; in all cases the standard deviation of fitting increased drastically, indicating very poor agreement between the experimental data and the model.

Using eqs 5 and 6, we determined the value of ΔH and K for p53 SS and SP peptides at different temperatures. Table 2 summarizes the results of the ITC experiments for these two peptides at pH 7.5. The temperature dependence of ΔH and ΔS is shown in Figures 3 and 4. Over the relatively narrow temperature range in which the experiments reported here were performed, ΔC_p can be treated as constant. The enthalpy and entropy change as a function of temperature are thus

$$\Delta H(T) = \Delta H_0 + \Delta C_p(T - T_0) \tag{7a}$$

$$\Delta S(T) = \Delta S_0 + \Delta C_p \ln (T/T_0) \tag{7b}$$

where ΔH_0 and ΔS_0 are the changes of enthalpy and entropy

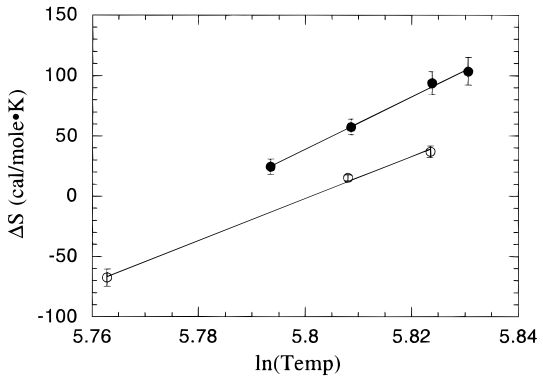

FIGURE 4: Temperature dependence of the tetramer dissociation entropy of p53 SS and SP peptides. The data were calculated from the values of ΔH and ΔG at each temperature; the filled circles are for the SP peptide and the open circles are for the SS peptide. The values of ΔC_p determined from this figure, according to eq 7b, were 2.2 kcal/(mol·K) for the SP peptide and 1.7 kcal/(mol·K) for the SS peptide, respectively.

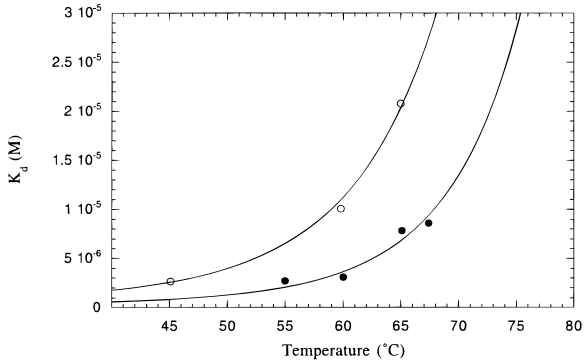

FIGURE 5: Tetramer dissociation constants of the p53 SS and SP peptide as functions of temperature. The filled circles represent the data for the SP peptide; the open circles are for the SS peptide. The values were calculated from the ΔG values.

at any reference temperature T_0. Accordingly, the heat capacities were independently determined from the slopes of the linear fitting in Figures 3 and 4. For the SS peptide, the values of ΔC_p were determined to be 1.6 and 1.7 kcal/(mol·K) from the temperature dependencies of ΔH and ΔS, respectively. For the SP peptide, the values of ΔC_p were 2.1 and 2.2 kcal/(mol·K), respectively. Since ΔH and ΔS are two independent variables in the statistical thermodynamic analysis, the excellent agreement between the ΔC_p values determined from ΔH and ΔS indicates the reliability of the data. Based on these parameter values and the definition of K_d in Table 1, we calculated the values of K_d shown in Figure 5 as a function of temperature. It is apparent that, at all temperatures, the value of K_d of the SP peptide is smaller than that of the SS peptide. This conclusion indicates enhanced tetramer stability by phosphorylation of Ser392, in agreement with the ultracentrifuge results.

To permit comparison with the ultracentrifuge data, the thermodynamic parameters determined by the ITC experiments were extrapolated to 30 °C as shown in Table 2, using eqs 2 and 7. Considering the propagated error of extrapolation, the values of ΔG and K_d are in reasonable agreement with those determined by ultracentrifugation. The values of the thermodynamic parameters were also calculated at 37 °C. For the SS peptide, these values were −9.3 kcal/mol for ΔH, 1.5 μM for K_d, and 1.6 kcal/(mol·K) for ΔC_p. For the SP peptide, these values are −3.5 kcal/mol, 0.5 μM, and

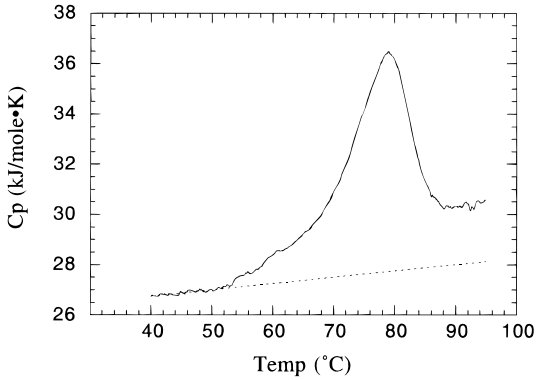

FIGURE 6: Partial molar heat capacity of the p53 SS peptide as a function of temperature. The experiment was performed at pH 7.5 in 50 mM sodium phosphate buffer with 0.1 M NaCl. The total peptide concentration was 100 μM, expressed as monomer. The dotted line represents the heat capacity of the folded peptide. The difference between the heat capacity before and after the peak corresponds to the heat capacity change of the transition. The unfolding is characterized by a transition temperature of 79.0 °C, an enthalpy change of 62.3 kcal/mol of tetramer and a ΔC_p of 1.6 kcal/(mol·K), respectively.

2.1 kcal/(mol·K) for ΔH, K_d, and ΔC_p, respectively. The 3-fold decrease of K_d for SP peptide is the result of a more favorable ΔG of 1.9 kcal/mol at 37 °C. In order to understand the mechanism of the stabilization of the tetramer by phosphorylation of Ser392, we have further examined the enthalpy and entropy changes shown in Table 2. It is apparent that the favorable ΔG of 1.9 kcal/mol upon phosphorylation was due to a favorable ΔH of 5.8 kcal/mol and an unfavorable contribution of 3.9 kcal/mol from the entropy term. This thermodynamic behavior is typical for the formation of polar interactions, such as hydrogen bonds, in protein folding and protein−peptide association (*39*). Therefore, the data, obtained calorimetrically, suggests that the tetramer stabilization by phosphorylation of Ser392 is achieved by the formation of new intra- or intermolecular polar interactions.

Differential Scanning Calorimetry. Previously it was shown that the monomeric form of p53 peptide has a disordered secondary structure and also has the absolute heat capacity of an unfolded peptide (*13*, *37*). This finding suggests that the dissociation of tetramer is accompanied by unfolding of the structure. Since DSC measures the thermodynamic parameters associated with a temperature-induced transition, folding/unfolding studies of p53 peptides performed in a DSC provide essentially the same information about tetramer dissociation as measurements by ITC. Figure 6 shows the heat capacity of the SS peptide as a function of temperature. The enthalpy and heat capacity change of the transition were determined by using the thermodynamic analysis described by Freire (*40*). At pH 7.5, the unfolding of the p53 SS tetramer is characterized by a transition temperature (T_m) of 79.0 °C, an enthalpy change of 62.3 kcal/mol of tetramer, and a heat capacity change of 1.6 kcal/(mol·K). The ΔH and ΔC_p values for the unfolding of the SP peptide are 80.8 kcal/mol at 79 °C and 2.2 kcal/(mol·K), respectively, while T_m is the same as that of the SS peptide. Table 3 shows a comparison of the results from DSC and ITC experiments. The values of ΔH obtained by the two methods for the peptides are in reasonably good agreement; the difference of approximately 5 kcal/mol is not unexpected for the different techniques. The agreement of the values

Table 3: Comparison of Thermodynamic Parameters between DSC and ITC Experiments at 65 °C

	DSC		ITC	
peptide	ΔH^a (kcal/mol)	$\Delta C_p{}^b$ (kcal/mol)	ΔH^b (kcal/mol)	$\Delta C_p{}^b$ (kcal/mol)
SS	39.9	1.6	34.6	1.6
SP	50.0	2.2	55.9	2.1

[a] Calculated from the enthalpy change at 65 °C using eq 7a. [b] Experimental values.

of ΔC_p is excellent. This agreement between these two different experimental approaches further supports the conclusion that the monomer is unfolded.

DISCUSSION

Seven 91 amino acid peptides, including both singly and doubly phosphorylated derivatives, comprising the C-terminal tetramerization and nonspecific DNA binding domains of human p53, were successfully synthesized by the segment condensation method using partially protected peptide thioesters (*33*). Since the thioester group is not nucleophilic yet still has the property of selective activation, the condensation method facilitated the efficient synthesis of the large peptide segment with high purity by minimizing the generation of side-reaction products.

From a point of view of a structure−function relationship, phosphorylation of p53 serine residues in the C-terminal domain could change the physical properties that affect the intrinsic DNA binding affinity of this protein and its stability as a tetramer. Since the functional DNA binding form of the protein is tetrameric, the change of either property will affect the regulatory functions of this molecule. In this work, we focused on the potential role of phosphorylation of the serines immediately flanking the tetramerization domain on the stability of the tetrameric form. We characterized the tetramer dissociation energetics of p53 C-terminal peptides (residues 303−393) in which different serines were phosphorylated, using analytical ultracentrifugation, titration calorimetry, and differential scanning calorimetry. Among the peptides with phosphorylated serine residues (Ser315, Ser378, and Ser392), only phosphorylation of Ser392 significantly enhanced tetramer stability, increasing the magnitude of ΔG by 2−4 kcal/mol. Phosphorylation of Ser315 or Ser378 had little effect, and it is noteworthy that when both Ser315 and Ser392 are phosphorylated, the stability of the peptide was virtually identical to that of the unphosphorylated peptide. This result suggests that phosphorylated Ser392 might interact with residues in the vicinity of Ser315 as a consequence of the antiparallel arrangement of the tetramer and that the enhanced stabilization resulting from the phosphorylation of Ser392 is attenuated by phosphorylation of Ser315. In agreement with these results, acetylation of the N-terminal α-amino group and the four ϵ-amino groups of lysine side chains also eliminates the stabilization resulting from the phosphorylation of Ser392, while acetylation of the unphosphorylated peptide had no effect on tetramer stability.

The results from calorimetry and analytical ultracentrifugation are consistent; both clearly indicate enhanced tetramer stabilization upon the phosphorylation of Ser392. This stabilization is characterized by a favorable enthalpy term and a less unfavorable entropy term at 37 °C, which results in a favorable ΔG of 1.9 kcal/mol of tetramer. Since such energetics are typical for the formation of hydrogen bonds in proteins, which have been estimated to have a ΔG of 0.5−1.5 kcal/mol per hydrogen bond in water (*41*−*43*), we suggest that the increased tetramer stabilization by phosphorylating Ser392 is the energetic consequence of forming 1−4 hydrogen bonds between the phosphorylated Ser392 and the *N*-terminal portion of the p53(303−393) peptide in the antiparallel dimer of dimers forming the tetramer.

Recently, Johnson et al. (*37*) have performed a differential scanning calorimetry study of the unfolding of a p53 peptide (residues 303−366) that includes the tetramerization domain. At pH 7.0 in phosphate buffer, the unphosphorylated peptide had a transition temperature of 84.8 °C. This is similar to what we observed for the SS peptide (79.0 °C) at pH 7.5. One should bear in mind that the peptides studied in our work have an additional 27 residues at the *C*-terminus when compared with the peptide studied by Johnson et al. (*37*). At 65 °C and pH 7.0, the unfolding of the 303−366 peptide is characterized by a ΔC_p of 1.7 kcal/(mol·K), a ΔG of 23.5 kcal/mol, and a ΔH of 110 kcal/mol or 15.7 cal/(g·K), calculated from Table 1 in Johnson et al. (*37*). Comparing these values with the values for the SS peptide in our Table 3, the two peptides exhibit a similar heat capacity change while having an enthalpy difference of 70 kcal/mol at 65 °C. The weight average ΔH for the SS peptide is 4.3 cal/(g·K), significantly lower than that of the 303−366 peptide. This enthalpy difference might be accounted for by the unfolding of the structures formed by the additional 27 residues on each peptide of the tetramer. Additionally, the free energy change of unfolding of the tetramer is very similar for both peptides; thus, the difference in enthalpy must be compensated by a change of entropy. Thus, the presence of the additional 27 residues in the SS peptide, which with the tetramerization domain comprise the nonspecific DNA binding domain of p53 (*12*), does not affect tetramer stability. This observation is also consistent with our earlier observation that peptides with residues 319−360 and 319−393 have very similar tetramer dissociation constants (*13*).

Within the 27 amino acid residues comprising the difference between our SS peptide (residues 303−393) and the peptide studied by Johnson et al. (residues 303−366) lies the PAb421 epitope (*44*). The monoclonal antibody PAb421 can activate sequence-specific DNA binding of unphosphorylated recombinant p53 (*22*). It also has been reported that the peptide (residues 369−383) derived from the C-terminal domain can activate sequence-specific DNA binding of p53 (*45*). The activation of DNA binding by this peptide is not strong; however, prior phosphorylation of Ser392 of the C-terminus by CKII significantly enhanced the DNA binding. These results suggested that the C-terminal flanking region interacts with the DNA binding domain on the tetramer and that this interaction can be disrupted by phosphorylation of Ser392. Our results demonstrate that the C-terminal flanking region could form polar interactions with the region in the vicinity of Ser315 as a result of the phosphorylation of Ser392. Thus, phosphorylation of Ser392 might allow the repositioning of the C-terminal region from the DNA binding domain to the region in the vicinity of Ser315. As results of this change, DNA binding to specific sites on the DNA binding domain is enhanced and p53 undergoes functional activation.

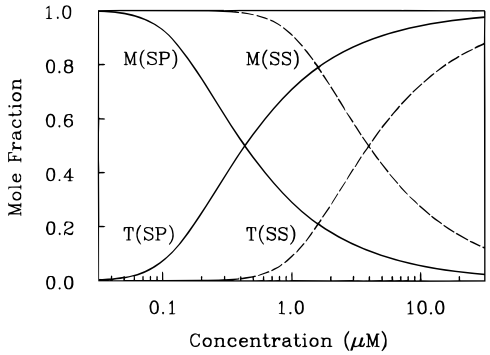

FIGURE 7: Mole fraction of monomer and tetramer as a function of total concentration expressed as moles of monomer for unphosphorylated p53(303−393) and for p53(303−393) with Ser392 phosphorylated. Monomer and tetramer are designated by M and T, respectively; SS (the dashed lines) refers to p53(303−393) with none of the serines phosphorylated and SP (the solid lines) refers to p53(303−393) with Ser392 phosphorylated. The equilibrium constants used for calculating the curves were given by $K_{14} = \exp(-\Delta G°/RT)$, using the values of $\Delta G°$ for SS and SP given in Table 1. It should be noted that the values of K_d, as given by the concentrations where the mole fractions of monomer and tetramer are equal, differ by a factor of 10.

In normal human cells with undamaged DNA, p53 cannot readily be detected by immunofluorescence in whole cells or in cell extracts by western blotting techniques; thus, its concentration is very low, probably of the order of 1000 molecules/cell or less. The volume of the nucleus of a human fibroblast is of the order of $(1-10) \times 10^{-13}$ L; thus the p53 concentration in the nucleus of normal human cells is of the order of 1−10 nM. If the K_d for intact wild-type p53 in the milieu of the nucleus at 37 °C is equivalent to that for the C-terminal domain, i.e., 1−10 μM, then virtually all of the p53 in normal cells will be monomeric and (comparatively) inactive with respect to sequence-specific DNA binding and transcriptional activation. Decreasing the K_d ~10-fold through phosphorylation of Ser392 coupled with a significant increase in the number of p53 molecules per nucleus (to perhaps ~50 000) would bring the p53 concentration into a range where tetramers form (Figure 7). Because of the fourth power relationship between monomer and tetramer concentrations coupled with a change in the dissociation constant, the transition between transcriptionally inactive and active p53 should occur over a relatively narrow concentration range. These considerations suggest that phosphorylation of C-terminal serines could provide a mechanism that contributes to the activation of p53 through phosphorylation of Ser392 and inactivates or prevents the activation of p53 through the phosphorylation of Ser315. Cell cycle-dependent phosphorylation of Ser315 also might function to prevent p53 activation under certain circumstances. While these considerations are speculative, they provide a framework in which to consider the role of posttranslational modifications in regulating p53 function, and they explain why previous studies of p53 phosphorylation site mutants, all of which involved highly overexpressed p53, failed to demonstrate a clear role for phosphorylation in p53 regulation (*46*, *47*).

In summary, several conclusions may be drawn from the thermodynamic analysis: (a) the peptide with phosphorylated Ser392 exhibits significantly enhanced stability and a more pronounced temperature dependence of the thermodynamic parameters; (b) calorimetry studies suggest that tetramer stabilization by the phosphorylation of Ser392 is achieved by formation of new polar interactions within the protein, possibly between Ser392 and residues adjacent to Ser315; and (c) phosphorylation of Ser315 or Ser378 have little effect on the tetramer stability.

REFERENCES

1. Levine, A. J. (1993) *Annu. Rev. Biochem. 62*, 623−651.
2. Murray, A. W. (1992) *Nature 359*, 599−604.
3. Hunter, T. (1993) *Cell 75*, 839−841.
4. Weinert, T., and Lydall, D. (1993) *Semin. Cancer Biol. 4*, 129−140.
5. Bates, S., and Vousden, K. H. (1996) *Curr. Opin. Genet. Dev. 6*, 12−19.
6. Gottlieb, T. M., and Oren, M. (1996) *Biochim. Biophys. Acta 1287*, 77−102.
7. Kastan, M. B., Onyekwere, O., Sidransky, D., Vogelstein, B., and Craig, R. W. (1991) *Cancer Res. 51*, 6304−6311.
8. Oren, M. (1994) *Semin. Cancer Biol. 5*, 221−227.
9. Ullrich, S. J., Anderson, C. W., Mercer, W. E., and Appella, E. (1992) *J. Biol. Chem. 267*, 15259−15262.
10. Meek, D. W. (1994) *Semin. Cancer Biol. 5*, 203−210.
11. Stenger, J. E., Mayr, G. A., Mann, K., and Tegtmeyer, P. (1992) *Mol. Carcinog. 5*, 102−106.
12. Wang, Y., Reed, M., Wang, P., Stenger, J. E., Mayr, G., Anderson, M. E., Schwedes, J. F., and Tegtmeyer, P. (1993) *Genes Dev. 7*, 2575−2586.
13. Sakamoto, H., Lewis, M. S., Kodama, H., Appella, E., and Sakaguchi, K. (1994) *Proc. Natl. Acad. Sci. U.S.A. 91*, 8974−8978.
14. Wang, P., Reed, M., Wang, Y., Mayr, G., Stenger, J. E., Anderson, M. E., Schwedes, J. F., and Tegtmeyer, P. (1994) *Mol. Cell. Biol. 14*, 5182−5191.
15. Pavletich, N. P., Chambers, K. A., and Pabo, C. O. (1993) *Genes Dev. 7*, 2556−2564.
16. Clore, G. M., Omichinski, J. G., Sakaguchi, K., Zambrano, N., Sakamoto, H., Appella, E., and Gronenborn, A. M. (1994) *Science 265*, 386−391.
17. Clore, G. M., Ernst, J., Clubb, R., Omichinski, J. G., Kennedy, W. M., Sakaguchi, K., Appella, E., and Gronenborn, A. M. (1995) *Nat. Struct. Biol. 2*, 321−333.
18. Lee, W., Harvey, T. S., Yin, Y., Yau, P., Litchfield, D., and Arrowsmith, C. H. (1994) *Nat. Struct. Biol. 1*, 877−890.
19. Jeffrey, P. D., Gorina, S., and Pavletich, N. P. (1995) *Science 267*, 1498−1502.
20. Halazonetis, T. D., and Kandil, A. N. (1993) *EMBO J. 12*, 5057−5064.
21. Pietenpol, J. A., Tokino, T., Thiagalingam, S., el, D. W., Kinzler, K. W., and Vogelstein, B. (1994) *Proc. Natl. Acad. Sci. U.S.A. 91*, 1998−2002.
22. Hupp, T. R., Meek, D. W., Midgley, C. A., and Lane, D. P. (1992) *Cell 71*, 875−886.
23. Hansen, S., Hupp, T. R., and Lane, D. P. (1996) *J. Biol. Chem. 271*, 3917−3924.
24. Hupp, T. R., and Lane, D. P. (1995) *J. Biol. Chem. 270*, 18165−18174.
25. Takenaka, I., Morin, F., Seizinger, B. S., and Klet, N. (1995) *J. Biol. Chem. 270*, 5405−5411.
26. Meek, D. W., Simon, S., Kikkawa, U., and Eckhart, W. (1990) *EMBO J. 9*, 3253−3260.
27. Addison, C., Jenkins, J. R., and Sturzbecher, H. W. (1990) *Oncogene 5*, 423−426.
28. Bischoff, J. R., Friedman, P. N., Marshak, D. R., Prives, C., and Beach, D. (1990) *Proc. Natl. Acad. Sci. U.S.A. 87*, 4766−4770.
29. Ullrich, S. J., Sakaguchi, K., Lees, M. S., Fiscella, M., Mercer, W. E., Anderson, C. W., and Appella, E. (1993) *Proc. Natl. Acad. Sci. U.S.A. 90*, 5954−5958.
30. Soussi, T., and May, P. (1996) *J. Mol. Biol. 260*, 813−818.
31. Oberosler, P., Hloch, P., Ramsperger, U., and Stahl, H. (1993) *EMBO J. 12*, 2389−2396.

32. Bakalkin, G., Yakovleva, T., Selivanova, G., Magnusson, K. P., Szekely, L., Kiseleva, E., Klein, G., Terenius, L., and Wiman, K. G. (1994) *Proc. Natl. Acad. Sci. U.S.A. 91*, 413−417.
33. Sakamoto, H., Kodama, H., Higashimoto, Y., Kondo, M., Lewis, M. S., Anderson, C. W., Appella, E., and Sakaguchi, K. (1996) *Int. J. Pept. Protein Res. 48*, 429−442.
34. Perkins, S. J. (1986) *Eur. J. Biochem. 157*, 169−180.
35. Wiseman, T., Williston, S., Brandts, J. F., and Lin, L. N. (1989) *Anal. Biochem. 179*, 131−137.
36. Privalov, G., Kavina, V., Freire, E., and Privalov, P. L. (1995) *Anal. Biochem. 232*, 79−85.
37. Johnson, C. R., Morin, P. E., Arrowsmith, C. H., and Freire, E. (1995) *Biochemistry 34*, 5309−5316.
38. Burrows, S. D., Doyle, M. L., Murphy, K. P., Franklin, S. G., White, J. R., Brooks, I., McNulty, D. E., Scott, M. O., Knutson, J. R., Porter, D., Young, P., and Hensley, P. (1994) *Biochemistry 33*, 12741−12745.
39. Murphy, K. P., and Freire, E. (1992) *Adv. Protein Chem. 43*, 313−361.
40. Freire, E. (1995) *Methods Mol. Biol. 40*, 191−218.
41. Pace, N. (1995) *Methods Enzymol. 259*, 538−554.
42. Kato, Y., Conn, M. M., and Rebek, J. J. (1995) *Proc. Natl. Acad. Sci. U.S.A. 92*, 1208−1212.
43. Habermann, S. M., and Murphy, K. P. (1996) *Protein Sci. 5*, 1229−1239.
44. Legros, Y., Lafon, C., and Soussi, T. (1994) *Oncogene 9*, 2071−2076.
45. Hupp, T. R., Sparks, A., and Lane, D. P. (1995) *Cell 83*, 237−245.
46. Fiscella, M., Zambrano, N., Ullrich, S. J., Unger, T., Lin, D., Cho, B., Mercer, W. E., Anderson, C. W., and Appella, E. (1994) *Oncogene 9*, 3249−3257.
47. Fuchs, B., O'Connor, D., Fallis, L., Scheidtmann, K. H., and Lu, X. (1995) *Oncogene 10*, 789−793.

BI970759W